

Dimetallaheteroborane clusters containing group 16 elements: A combined experimental and theoretical study

KIRAN KUMARVARMA CHAKRAHARI, RONGALA RAMALAKSHMI, DUDEKULA SHARMILA and SUNDARGOPAL GHOSH*

Department of Chemistry, Indian Institute of Technology Madras, Chennai 600 036, India
e-mail: sghosh@iitm.ac.in

MS received 2 April 2014; accepted 4 August 2014

Abstract. Recently we described the synthesis and structural characterization of various dimetallaheteroborane clusters, namely *nido*-[(Cp*Mo)₂B₄ECl_xH_{6-x}], **1–3**; (**1**: E = S, x = 0; **2**: E = Se, x = 0; **3**: E = Te, x = 1). A combined theoretical and experimental study was also performed, which demonstrated that the clusters **1–3** with their open face are excellent precursors for cluster growth reaction. In this investigation process on the reactivity of dimetallaheteroboranes with metal carbonyls, in addition to [(Cp*Mo)₂B₄H₆EFe(CO)₃] (**4**: E = S, **6**: E = Te) reported earlier, reaction of **2** with [Fe₂(CO)₉] yielded mixed-metallaselaborane [(Cp*Mo)₂B₄H₆SeFe(CO)₃], **5** in good yield. The quantum chemical calculation using DFT method has been carried out to probe the bonding, NMR chemical shifts and electronic properties of dimolybdaheteroborane clusters **4–6**.

Keywords. Metallaborane; DFT study; organometallic; cluster

1. Introduction

In the recent past, the reactivity of metallaheteroboranes^{1–13} has made great advances, particularly in macro-polyhedral systems.¹⁴ The chalcogenoheteroboranes and their metallo derivatives are restricted to thio derivatives with no well known examples in seleno or telluroheteroborane chemistry. The reactivity and stability of chalcogenoheteroboranes considerably deviates from their parent metallaboranes.^{15–18} For example, the chemistry of transition metal complexes with chalcogen ligands is of enormous impact to a wide range of chemical, engineering and natural systems.¹⁹ Recently, we have demonstrated that compounds of the type [(Cp*Mo)₂B₄E₂H₄],² (E = S, Se and Te) are useful metal synthons for cubane-type clusters.⁵ Further, a combined theoretical (density functional theory (DFT)) and experimental study reveals that the reactivity of dimolybdaborane [(Cp*Mo)₂B₅H₉]²⁹ with various metal carbonyls increases upon the replacement of one of the open face boron vertices by chalcogen atoms. In this process, we have reported a variety of dimetallaheteroborane clusters, viz., *nido*-[(Cp*Mo)₂B₄ECl_xH_{6-x}], **1–3**; (**1**: E = S, x = 0; **2**: E = Se, x = 0; **3**: E = Te, x = 1)^{20–23} and tested their reactivity with di-nuclear metal carbonyl compounds. For example, the reaction of **3** with [Co₂(CO)₈] at room

temperature yielded a byproduct which is a member of a novel class of triple-decker complexes.²³ As a part of our continuing exploration on metallaheteroboranes and their derivatives, we recently synthesized and isolated the S, Se, Te analogues of dimetallaheteroborane clusters and we are also fascinated by the reactivity of those clusters with metal carbonyls.^{22–24} In our previous results we have shown that the reaction between [Cp*MoCl₄] and [LiBH₄.thf], with potential chalcogen sources yielded compounds **1–3**, similar to the parent metallaborane [(Cp*Mo)₂B₅H₉].²⁹ The geometries, structure, stabilities and electronic structures of these clusters investigated using density functional theory (DFT) method.

2. Experimental

2.1 General procedures and instrumentation

All the operations were conducted under an Ar/N₂ atmosphere using standard Schlenk techniques. Solvents were distilled prior to use under Argon. MeI was freshly distilled prior to use. All other reagents Cp*H, [Mo(CO)₆], BuLi, BH₃.thf, Se powder, LiBH₄ 2.0 M in thf, [Fe₂(CO)₉] (Aldrich) were used as received. [(η⁵-C₅Me₅)MoCl₄] was prepared with some modification²⁶ of Green's²⁷ work. Thin layer chromatography was carried on 250 mm dia aluminum supported

*For correspondence

silica gel TLC plates (MERCK TLC Plates). The NMR spectra were recorded on 400 and 500 MHz Bruker FT-NMR spectrometer. Residual solvent protons were used as reference (δ , ppm, CDCl_3 , 7.26), while a sealed tube containing the external reference for ^{11}B NMR, $[\text{Bu}_4\text{N}(\text{B}_3\text{H}_8)]^{28}$ and $[(\eta^5\text{-C}_5\text{Me}_5\text{Mo})_2\text{B}_5\text{H}_9]^{29}$ were synthesized with literature methods. Infrared spectra were obtained on a Nicolet 6700 FT-IR spectrometer. Microanalyses for C, H and N were performed on Perkin Elmer Instruments series II model 2400.

2.2 Synthesis of 5

In a flame-dried Schlenk tube, a hexane solution of **2** (0.2 g, 0.37 mmol) was added to $[\text{Fe}_2(\text{CO})_9]$ (0.13 g, 0.36 mmol) at room temperature and stirred for 6 h. Then, volatiles were removed *in vacuo* and the resulting brown residue was extracted with hexane and passed through Celite. The filtrate was concentrated and kept at -40°C to remove $[\text{Fe}_3(\text{CO})_{12}]$. The mother liquor was concentrated, and the residue was chromatographed on silica gel TLC plates. Elution with hexane: CH_2Cl_2 (95:05 *v/v*) mixture afforded green $[(\text{Cp}^*\text{Mo})_2\text{B}_4\text{H}_6\text{SeFe}(\text{CO})_3]$, **5** (0.08 g, 32%).

5: ^{11}B NMR (128 MHz, CDCl_3 , 22°C): δ 85.9 (d, $J_{\text{B-H}} = 133$ Hz, 2B), 44.9 (d, $J_{\text{B-H}} = 132$ Hz, 1B), -4.9 (d, $J_{\text{B-H}} = 138$ Hz, 1B); ^1H NMR (400 MHz, CDCl_3 , 22°C): δ 8.21 (br, 2B- H_t), 4.72 (br, 1B- H_t), 1.91 (s, 30H, Cp^*), 1.36 (br, B- H_t), -15.36 (br, 2Mo- H-B); ^{13}C NMR (100 MHz, CDCl_3 , 22°C): δ 215.2, 205.2 (s, CO), 104.3 (s, $\eta^5\text{-C}_5\text{Me}_5$), 11.3 (s, $\eta^5\text{-C}_5\text{Me}_5$); IR (hexane, cm^{-1}): 2493 (w) (B- H_t), 2015 (s), 1962 (s) ν (C-O). Anal. Calcd for $\text{C}_{23}\text{H}_{37}\text{B}_6\text{FeMo}_2\text{O}_3\text{Se}$: C, 44.12; H, 5.58. Found: C, 44.27; H, 5.63.

2.3 Single-crystal structure determination

Crystal data for **5** was collected and integrated using Bruker Apex II CCD area detector system equipped with graphite monochromated Mo- $\text{K}\alpha$ ($\lambda = 0.71073$ Å) radiation at 293K. The structure was solved by heavy atom methods using SHELXS-97³⁰ and refined using SHELXL-97³¹. The structure with the atom numbering scheme is shown in figure 1 and the crystallographic data for compound **5** is summarized in table 1.

3. Result and Discussion

3.1 Synthesis and characterization of 5

In our earlier communication we described the reaction of an air and moisture sensitive intermediate, obtained

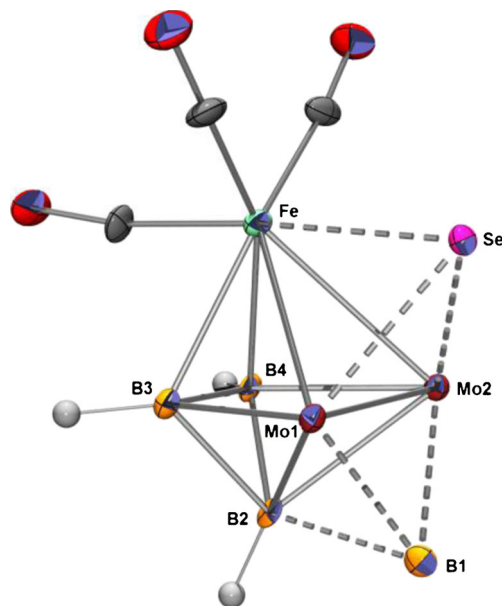


Figure 1. Molecular structure and labelling diagram for $[(\text{Cp}^*\text{Mo})_2\text{B}_4\text{H}_6\text{SeFe}(\text{CO})_3]$, **5**. Cp^* ligands are not shown for clarity. Selected bond lengths [Å] and angles [$^\circ$]: Mo(1)-Mo(2) 2.9189(14), Mo(1)-B(1) 2.261(16), Mo(1)-B(2) 2.412(12), Mo(1)-B(3) 2.164(15), Mo(1)-Se(1) 2.4941(17), Mo(1)-Fe(1) 2.796(2), Fe(1)-Se(1) 2.455(2), B(1)-B(2) 1.91(2), B(3)-Fe(1) 2.206(14), B(3)-Mo(1)-B(1) 92.6(6), B(1)-Mo(1)-Fe(1) 106.5(4), B(3)-Mo(1)-Mo(2) 75.0(5).

from the reaction of $[\text{Cp}^*\text{MoCl}_4]$ and $\text{LiBH}_4\cdot\text{thf}$, with other potential chalcogen sources yielded *nido*- $[(\text{Cp}^*\text{Mo})_2\text{B}_4\text{ECl}_x\text{H}_{6-x}]$, **1-3**; (**1**: E = S, $x = 0$; **2**: E = Se,

Table 1. Crystal data and structure refinement details for compound **5**.

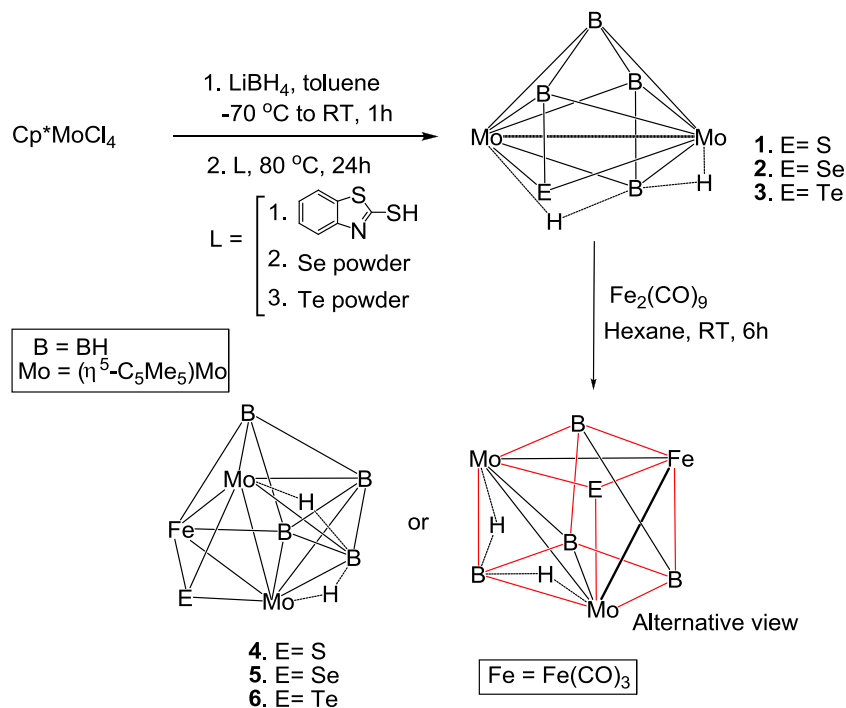
Empirical formula	$\text{C}_{23}\text{H}_{33}\text{B}_4\text{FeMo}_2\text{O}_3\text{Se}$, 5
Formula weight	727.42
Temperature (K)	298(2)
Crystal system	Orthorhombic
Space group	Fdd2
Unit cell dimensions	
a (Å)	25.063(2)
b (Å)	24.5106(16)
c (Å)	18.2711(10)
α ($^\circ$)	90.00
β ($^\circ$)	90.00
γ ($^\circ$)	90.00
V (Å ³)	11224.1(14)
Z	16
Dcalc (Mg/m ³)	1.722
F (000)	5744
μ (mm ⁻¹)	2.710
θ Range ($^\circ$)	1.61–28.35
Goodness-of-fit	1.064
R1, wR2 [$I > 2\sigma(I)$]	0.0759, 0.2099
R1, wR2 (all data)	0.0983, 0.2250
Largest diff. peak, hole ($e/\text{Å}^3$)	2.178, -1.518

$x = 0$; **3**: E = Te, $x = 1$) compounds.^{20–23} The dimolybdaheteroboranes **1–3**, was found to be very reactive towards metal carbonyl compound and as a result, room temperature reaction of **1–3**, with $[\text{Fe}_2(\text{CO})_9]$ yielded bicapped octahedral geometry complexes $[(\text{Cp}^*\text{Mo})_2\text{B}_4\text{H}_6\text{EFe}(\text{CO})_3]$, (**4**: E = S, **5**: E = Se, **6**: E = Te). The mass spectrometric data of **5** corresponds to $[(\text{Cp}^*\text{Mo})_2\text{B}_4\text{H}_6\text{SeFe}(\text{CO})_3]$ and the NMR spectroscopic data of the isolated solids are consistent with the formulation of **5**. As shown in scheme 1, room temperature reaction of $[(\text{Cp}^*\text{Mo})_2\text{B}_4\text{SeH}_6]$ ²², with $\text{Fe}_2(\text{CO})_9$ yielded **5**. This reaction also produced few other products, which were observed during the chromatographic work-up. However, isolation and characterization were not possible due to insufficient amounts. Note that compounds **1–4** and **6** have been reported earlier.^{20–23}

Compound **5** was isolated as a green solid in 32% yield. The spectroscopic data of **5** is comparable to that of **6** and is $[(\text{Cp}^*\text{Mo})_2\text{B}_5\text{H}_9\text{Fe}(\text{CO})_3]$ reported earlier²⁵ and is consistent with its solid state structure (determined by X-ray diffraction). Three types of resonances were observed in the ^{11}B NMR spectrum at δ 85.9, 44.9 and -4.9 (2:1:1) and the $^1\text{H}\{^{11}\text{B}\}$ NMR spectrum reveals three types of B-H protons in the ratio of 2:1:1 and the presence of one high-field ^1H resonance at δ -14.41 ppm of intensity 2. The ^1H NMR data suggest a plane of symmetry for a static molecule as well as the presence of single Cp^* resonance at 1.91 ppm of relative

intensity 30. The ^{13}C NMR spectrum contains signals attributable to one type of Cp^* ligand and $\text{Fe}(\text{CO})_3$ fragment. The IR spectrum shows a band at 2493 cm^{-1} in a region characteristic of the B-H stretching frequency and two more strong bands at 2015 and 1962 cm^{-1} which are assigned to the CO stretching modes of the $\text{Fe}(\text{CO})_3$ group.

The existence of compound **5** permits structural comparison with S and Te analogues without perturbations caused by additional metal fragments or ligands. The important geometrical differences among the bicapped octahedral cores of $[(\text{Cp}^*\text{Mo})_2\text{B}_4\text{H}_6\text{E}]$ (E = S, Se, Te and BH_3) are shown in chart 1 and table 2. As the geometries of all these clusters are same, differences are sought in the magnitude of the structural parameters and the NMR chemical shifts. Dihedral angle between the two capping triangular faces Mo-Mo-B and Mo-Mo-E for complex $[(\text{Cp}^*\text{Mo})_2\text{B}_4\text{H}_6\text{EFe}(\text{CO})_3]$ increases as E changes from BH_3 , S, Se and Te. On the other hand, there is a gradual increase in Mo-Mo bond length from 2.88–2.95 Å as E changes from S, Se and Te. The significant lengthening of the Mo-Mo bond length from S to Te might arise from both the size and electronegativity effect of S vs. Te. The distance between the two capping boron atoms of $[(\text{Cp}^*\text{Mo})_2\text{B}_4\text{H}_6\text{SeFe}(\text{CO})_3]$ (3.45 Å) is in between those of its S (3.30 Å) and Te (3.55 Å) analogues. The observed ^1H and ^{11}B NMR chemical shift correlation of **5** with S and Te analogues



Scheme 1. Synthesis of dimolybdaheteroborane, $[(\text{Cp}^*\text{Mo})_2\text{B}_4\text{EH}_6]$, **1–3** and $[(\text{Cp}^*\text{Mo})_2\text{B}_4\text{H}_6\text{EFe}(\text{CO})_3]$, **4–6**. Note: Compounds **1–3**, **4** and **6** have been reported earlier.

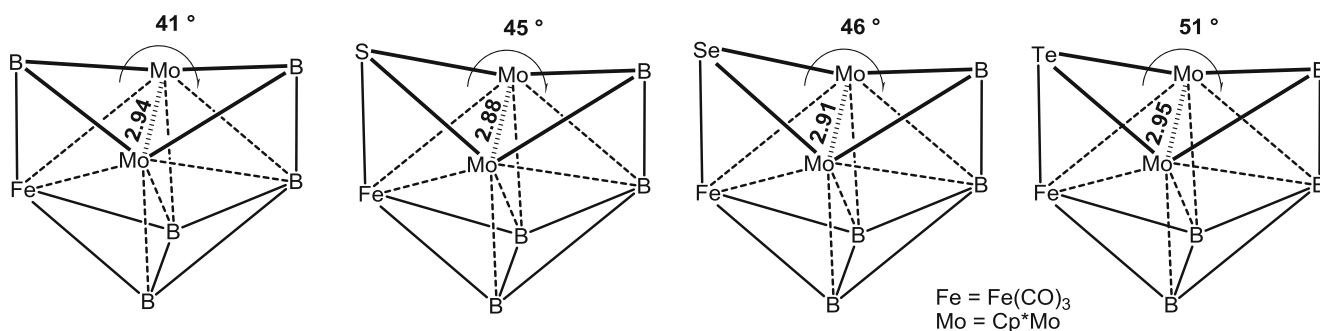


Chart 1. Dihedral angles and M-M bond lengths of $[(\text{Cp}^*\text{Mo})_2\text{B}_4\text{H}_6\text{EFe}(\text{CO})_3]$ ($\text{E} = \text{S}, \text{Se}, \text{Te}, \text{BH}_3$). Hydrogens are not shown for clarity.

may be due to perturbation of the electronic environment of the boron atoms by the chalcogen. On going from the lighter to the heavier chalcogen atom, the ^1H (Mo-H-B protons) and ^{11}B NMR (both capping and $\text{M}_2\text{B}_3\text{Fe}$ octahedral boron atoms) resonances appear at low field.

Single crystals suitable for X-ray diffraction analysis of **5** were obtained from a hexane/ CH_2Cl_2 solution at -5°C , thus allowing the structural characterization of **5**. The solid state X-ray structure of **5** (figure 1) is best viewed as a bicapped octahedron $\{\text{Mo}_2\text{B}_4\text{FeSe}\}$, with Mo1, Mo2, B2, B3, B4 and Fe occupying the vertices of the core octahedron, in which the faces Mo1-Mo2-Fe and Mo1-Mo2-B2 are capped by Se and B1, respectively. The structure and spectroscopic data of **5** is very similar to that of $[(\text{Cp}^*\text{M})_2\text{B}_5\text{H}_9\text{Fe}(\text{CO})_3]$ ($\text{M} = \text{Mo}, \text{W}$) (table 2). The capped BH_3 group in $[(\text{Cp}^*\text{M})_2\text{B}_5\text{H}_9\text{Fe}(\text{CO})_3]$ is substituted by isoelectronic $\mu_3\text{-Se}$ and maintains the same number of cluster valence electrons. The change from the bicapped trigonal bipyramidal geometry observed for the seven-sep species **1–3** to the bicapped octahedron observed for **4–6** is entirely in keeping with the changes predicted by Wade/Mingos rules for the addition of a two-electron three orbital fragment, such as $\text{Fe}(\text{CO})_3$. The Mo-Mo bond length in **5** is somewhat longer than that found in $[(\text{Cp}^*\text{Mo})_2\text{B}_4\text{SeH}_5(\text{Ph})]$ (2.88 \AA as opposed to 2.81 \AA). There are only a few examples of metallaboranes with bicapped octahedral geometry

known; $[(\text{Cp}^*\text{M})_2\text{B}_5\text{H}_9\text{Fe}(\text{CO})_3]$ ($\text{M} = \text{Mo}, \text{W}$), $[(\text{Cp}^*\text{W})_2\text{B}_6\text{H}_{10}]$,^{25,32} *closo*-2,3- $[(\text{Cp}^*\text{Ru})_2\text{B}_6\text{H}_3\text{Cl}_3]$ ³³ and $[\text{Cp}_3^*\text{Ru}_2\text{IrB}_5\text{H}_5]$.³⁴

3.2 Quantum chemical calculations

We have analyzed the incongruity in reactivity of the chalcogenato metallaborane clusters with $[\text{Fe}_2(\text{CO})_9]$ in comparison to their parent metallaboranes, by using density functional theory (DFT) study. Further, with the help of DFT study, we have analyzed the variation of stability of the model compounds $[(\text{Cp}^*\text{M})_2\text{B}_5\text{H}_9\text{Fe}(\text{CO})_3]$, **4a**, **5a** and **6a** (Cp analogues of $(\text{Cp}^*\text{M})_2\text{B}_5\text{H}_9\text{Fe}(\text{CO})_3$, **4**, **5**, and **6** respectively). DFT calculations were carried out in order to determine the electronic factors such as (i) the molecular orbital analysis (ii) the bond length between two metals, (ii) the position of bridging and terminal hydrogen atoms, and (iv) the spectroscopic properties (^{11}B and ^1H NMR chemical shifts) of these molecules.

3.2a Geometry optimizations: Significant bond lengths for the all-electron in gaseous state (no solvent effect) without any symmetry constraints at B3LYP/def2-TZVP optimized geometries, along with the experimentally obtained structural parameters, are given in table S1. The calculated bond parameters are slight disparity from the experimentally measured

Table 2. Selected structural parameters and ^{11}B NMR data of **5** and other related compounds.

Metallaborane	d(M-M) [Å]	$d_{\text{avg}}(\text{M-B})$ [Å]	d(B-B) [Å]	^{11}B NMR δ [ppm]	Ref.
5	2.91	2.25	1.79	85.9, 44.9, -4.9	-
4	2.88	2.23	1.77	86.7, 44.7, -5.3	15
6	2.95	2.32	1.74	85.6, 45.6, -4.0	16
$[(\text{Cp}^*\text{Mo})_2\text{B}_5\text{H}_9\text{Fe}(\text{CO})_3]$	2.94	2.27	1.75	90.4, 41.4, 29.7, -0.4	20
$[(\text{Cp}^*\text{W})_2\text{B}_5\text{H}_9\text{Fe}(\text{CO})_3]$	2.93	2.28	1.79	84.2, 46.2, 39.1, -6.6	27
$[(\text{Cp}^*\text{W})_2\text{B}_6\text{H}_{10}]$	2.95	2.28	1.77	83.9, 47.9, -12.7	27

for all the compounds. For example the experimentally observed Mo–Mo distance of 2.941 Å in $[(\text{Cp}^*\text{Mo})_2\text{B}_5\text{H}_9\text{Fe}(\text{CO})_3]$, slightly deviates to the calculated one (2.971 Å). Similarly, the computed Mo–Mo distances for compounds **4a**, **5a** and **6a** (2.920, 2.947 and 2.982 Å respectively) deviate from the experimentally observed values (2.885, 2.919, and 2.952 Å, respectively). The geometry optimization of **5a** at the B3LYP/def2-TZVP for all-electron level shows an Mo–Mo bond length of 2.947 Å, which is significantly longer than the solid state structure bond parameter's observed value of 2.919 (7) Å.

3.2b Electronic structure analysis: To understand the electronic structure of $[(\text{CpMo})_2\text{B}_5\text{H}_9\text{Fe}(\text{CO})_3]$, **4a**, **5a** and **6a** the DFT studies have been carried out and analyzed. The HOMO-LUMO energy gap (ca. 3 eV) at the B3LYP level calculated for $[(\text{CpMo})_2\text{B}_5\text{H}_9\text{Fe}(\text{CO})_3]$, **4a**, **5a** and **6a** shows reasonable agreement with the experimentally observed stabilities of these complexes. Note, a destabilization of the HOMO-LUMO has been found in chalcogenato metallaborane compounds (**4a–5a**) compared to their parent metallaborane $[(\text{Cp}^*\text{M})_2\text{B}_5\text{H}_9\text{Fe}(\text{CO})_3]$, which shows some narrow stabilization of the HOMO leading to a slighter HOMO-LUMO gap. In general, for this kind of cage cluster, a strong delocalization over the whole molecule is observed from the composition analysis of the MO

located in the HOMO region. This may be due to the introduction of π -donor chalcogens into the clusters^{18,19} (figure 2). The HOMO-LUMO gap for $[(\text{Cp}^*\text{Mo})_2\text{B}_4\text{H}_6\text{SeFe}(\text{CO})_3]$ (3.469 eV) is smaller than its analogues molybdaborane complex **4a**, (3.569 eV), larger than its analogues molybdaborane complex **6a** (3.290 eV) and the gap decreases as the chalcogen atom gets heavier (table S2). Further, The Wiberg Bond Index (WBI)³⁵ value 0.59 of **5** supports the existence of a Mo–Mo cross cluster bond in HOMO (figure S1)

3.2c Ionization potentials: The ionization potential (IP) energies are a reasonable precursor of the metal-boron cage stability, has been calculated for all the model compounds. Both the DFT-computed vertical and adiabatic first IPs are shown in figure 3. The computed IP values are above 6.0 eV, which suggest the high thermodynamical stability of the compounds (**4a–6a**). The vertical curve is a few tenths of an electron volt higher in energy, compared to the adiabatic IP, because of the significant geometry change upon ionization.

3.2d NMR chemical shifts: In addition, ¹¹B and ¹H chemical shift calculation of **4a–6a** (Cp analogue of **4–6**), using gauge-independent atomic orbital density functional theory [GIAO-DFT] method at B3LYP/

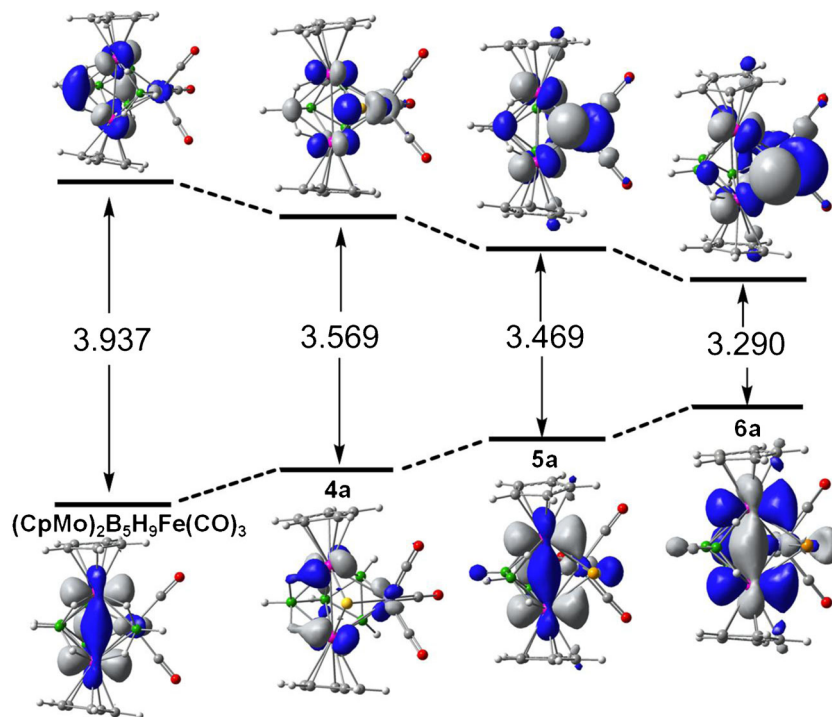


Figure 2. Frontier molecular orbital (MO) diagram of $[(\text{CpMo})_2\text{B}_5\text{H}_9\text{Fe}(\text{CO})_3]$, **4a**, **5a** and **6a** (LUMO-top, HOMO-bottom).

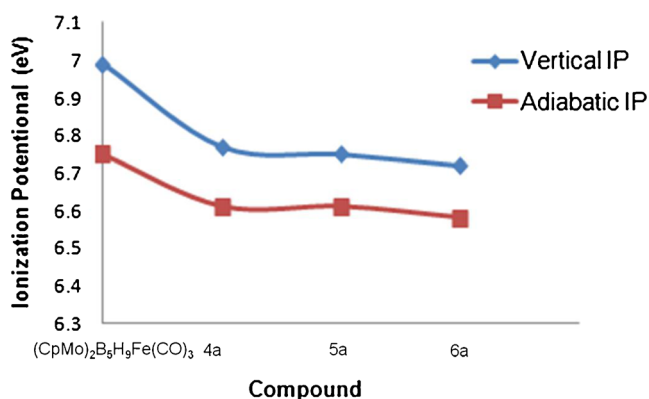


Figure 3. Vertical and adiabatic first ionization potentials (IPs, in eV) for compounds [(CpMo)₂B₅H₉Fe(CO)₃], **4a–6a** computed at the B3LYP/def2-TZVP level.

def-TZVP level referenced to BF₃·OEt₂ and IR data are satisfactory matches to the experimental values (table S3). This indeed provides a stringent test to the validity of the calculated electronic structures of the complexes **4–6**.

4. Conclusion

Various dimetallaheteroborane clusters, namely *nido*-[(Cp*Mo)₂B₄ECI_xH_{6-x}], **1–3**; (**1**: E = S, x = 0; **2**: E = Se, x = 0; **3**: E = Te, x = 1), have been reacted with Fe₂(CO)₉ which yielded [(Cp*Mo)₂B₄H₆EFe(CO)₃], (E = S, Se, and Te) in good yields. Compounds **1–4** and **6** have been reported earlier. The experimental results were accompanied and rationalized by means of the DFT studies, which reveal geometries in agreement with the structure determinations. Further, the DFT study illustrates the stabilities of these clusters. Although a few examples of metallaboranes with bicapped octahedral geometry are known, as per our knowledge, cluster **4, 5, 6** are the first examples of metallaheteroborane with this geometry.

Supplementary Information

The supporting information contents include optimized geometries for compounds [(CpM)₂B₅H₉Fe(CO)₃] **4a–6a** (Cp analogues of [(Cp*Mo)₂B₅H₉Fe(CO)₃], **4–6** respectively), comparative NMR table (table S3) and other supplementary information (bond parameters, HOMO-LUMO energy gap). Crystallographic data for the structural analysis has been deposited with the Cambridge Crystallographic Data Centre, CCDC 905304 for compounds **5**. Copies of this information may be obtained free of charge from the Director, CCDC, 12 Union Road, Cambridge CB2 1EZ, UK;

Fax: (+44) 1223-336-033; or e-mail: deposit@ccdc.cam.ac.uk or via www.ccdc.cam.ac.uk/conts/retrieving.html.

Acknowledgements

Generous support of the Council of Scientific and Industrial Research (Grant No. 01(2422)/10/EMR-II), New Delhi is gratefully acknowledged. KKC and RR thank the University Grants Commission (UGC) for fellowships and DS is grateful to the Council of Scientific and Industrial Research (CSIR), India for fellowship. We thank V Ramkumar for X-ray crystallography analysis.

References

- Dhayal R S, Chakrahari K K V, Ramkumar V and Ghosh S 2009 *J. Clust. Sci.* **20** 565
- Sahoo S, Mobin S M and Ghosh S 2010 *J. Organomet. Chem.* **695** 945
- Dhayal R S, Chakrahari K K V, Varghese B, Mobin S M and Ghosh S 2010 *Inorg. Chem.* **49** 7741
- Chakrahari K K V, Dhayal R S and Ghosh S 2011 *Polyhedron* **30** 1048
- Geetharani K, Bose S K, Sahoo S and Ghosh S 2011 *Angew. Chem. Int. Ed.* **50** 3908
- Bose S K, Geetharani K, Varghese B and Ghosh S 2011 *Inorg. Chem.* **50** 2445
- Chakrahari K K V, Mobin S M and Ghosh S 2011 *J. Clust. Sci.* **22** 149
- Bose S K, Geetharani K, Ramkumar V, Varghese B and Ghosh S 2010 *Inorg. Chem.* **49** 2881
- Ghosh S, Fehlner T P and Noll B C 2005 *Chem. Commun.* 3080
- Ghosh S, Lei X, Shang M and Fehlner T P 2000 *Inorg. Chem.* **39** 5373
- Roy D K, Bose S K, Anju R S, Mondal B, Ramkumar V and Ghosh S 2013 *Angew. Chem. Int. Ed.* **52** 3222
- Roy D K, Bose S K, Geetharani K, Chakrahari K K V, Mobin S M and Ghosh S 2012 *Chem. Eur. J.* **18** 9983
- Sahoo S, Reddy K H K, Dhayal R S, Mobin S M, Ramkumar V, Jemmis E D and Ghosh S 2009 *Inorg. Chem.* **48** 6509
- Kim D Y and Girolami G S 2006 *J. Am. Chem. Soc.* **128** 10969
- Bose S K, Geetharani K, Varghese B and Ghosh S 2010 *Inorg. Chem.* **49** 6375
- Dhayal R S, Sahoo S, Reddy K H K, Mobin S M, Jemmis E D and Ghosh S 2010 *Inorg. Chem.* **49** 900
- Dhayal R S, Ramkumar V and Ghosh S 2011 *Polyhedron* **30** 2062
- Ghosh S, Rheingold A L and Fehlner T P 2001 *Chem. Commun.* 895
- Stadelman B S and Brumaghim J L 2013 *ACS Symposium Series* **1152** Chapter 3, pp 33
- Chakrahari K K V and Ghosh S 2011 *J. Chem. Sci.* **123** 847
- Thakur A, Sao S, Ramkumar V and Ghosh S 2012 *Inorg. Chem.* **51** 8322

22. Chakrahari K K V, Thakur A, Mondal B, Ramkumar V and Ghosh S 2013 *Inorg. Chem.* **52** 7923
23. Thakur A, Chakrahari K K V, Mondal B and Ghosh S 2013 *Inorg. Chem.* **52** 2262
24. Krishnamoorthy B S, Thakur A, Chakrahari K K V, Bose S K, Hamon P, Roisnel T, Kahlal S, Ghosh S and Halet J-F 2012 *Inorg. Chem.* **51** 10375
25. Aldridge S, Hashimoto H, Kawamura K, Shang M and Fehlner T P 1998 *Inorg. Chem.* **37** 928
26. Dhayal R S, Sahoo S, Ramkumar V and Ghosh S 2009 *J. Organomet.Chem.* **694** 237
27. Green M L H, Hubert J D and Mountford P 1990 *J. Chem. Soc., DaltonTrans.* 3793
28. Ryschkewitsch G E and Nainan K C 1975 *Inorg. Synth.* **15** 113
29. Aldridge S, Fehlner T P and Shang M 1997 *J. Am. Chem. Soc.* **119** 2339
30. Sheldrick G M 1997 SHELXS-97, A program for solution of crystal structures, University of Göttingen, Germany
31. Sheldrick G M 1997 SHELXL-97, A program for solution of crystal structures, University of Göttingen, Germany
32. Bose S K, Ghosh S, Noll B C, Halet J-F, Saillard J-Y and Vega A 2007 *Organometallics* **26** 5377
33. Ghosh S, Fehlner T P, Beatty A M and Noll B C 2005 *Organometallics* **24** 2473
34. Mavunkal I J, Noll B C, Meijboom R, Muller A and Fehlner T P 2006 *Organometallics* **25** 2906
35. Wiberg K 1968 *Tetrahedron* **24** 1083